Chapter 5

Deciphering molecular mechanism of anticancer compound abemaciclib on underlying antileishmanial activities

Abstract

Despite numerous endeavors, currently, available therapeutics for leishmaniasis remain insufficiently effective, characterized by high costs, adverse side effects, limited efficacy, painful routes of administration, absence of approved vaccines, and the emergence of parasite resistance. These challenges underscore the urgent need to discover new medications to combat this neglected tropical disease. In this context, drug repurposing emerges as a promising strategy. Here, we have delved into the molecular mechanisms underlying the antileishmanial activities of the anticancer drug Abemaciclib. This compound has exhibited leishmanicidal effects in the micromolar range against both forms of the leishmania parasite while demonstrating minimal toxicity against macrophages. Electron microscopy revealed distinct morphological changes in Abemaciclib-treated parasites, including cell rounding, shrinkage, and loss of flagella. Fluorescence microscopy staining with MitoSox red and DAPI further indicated disruption of mitochondrial structure, enlargement of nuclear structure, and loss of kinetoplast. Moreover, flow cytometric analysis unveiled increased reactive oxygen species (ROS) production, mitochondrial membrane potential depolarization, elevation in sub-G1 cell population, and DNA fragmentation as observed in DNA laddering assays. These characteristics indicate apoptotic cell death, a notion corroborated by flow cytometric analysis of Abemaciclib-treated cells stained with Annexin-V and PI, revealing that 64% of cells were in an apoptotic state. In summary, Abemaciclib demonstrates leishmanicidal activity through apoptotic cell death pathways, presenting itself as a promising lead molecule for the treatment of this debilitating disease**.**

Key words: Antileishmanial drug, Abemaciclib, Apoptosis, Leishmaniasis, oxidative stress.

Part of the chapter has been published in the **Journal of Cellular Biochemistry**, **2023**, 124(9), 1402-1422.

5.1 Introduction

When it comes to drug discovery, leishmaniasis stands as a neglected tropical disease. Yet, its impact affects millions worldwide, with regions of social and economic vulnerability bearingzz the brunt of its severity [Islamuddin et al., 2022]. Presently, chemotherapeutics such as Pentavalent antimonies, Amphotericin B, Paromomycin, Miltefosine, and Pentamidine, either alone or in combination, represent the primary treatment options for various forms of leishmaniasis. However, these treatments are not entirely effective and have several limitations, including efficacy, toxicity, prolonged duration of action, high cost, and the emergence of resistant parasites. This scenario underscores the urgent need to discover new therapeutics with different mechanisms of action, increased potency, shorter treatment cycles, affordability, and accessibility in endemic regions. Various drug discovery approaches have been explored in this context, with drug repurposing emerging as a particularly promising avenue. This approach is recognized for its cost-effectiveness and expedited timeline in uncovering new treatments for parasitic diseases like leishmaniasis [da Silva Rodrigues et al., 2019].

Abemaciclib is a 2-anilino-2,4-pyrimidine derivative and an active ingredient of Verzenio, commercialized by Eli Lilly and Co. It is an antitumor agent and a dual inhibitor of cyclin-dependent kinases 4 (CDK4) and 6 (CDK6) [Voli et al., 2020]. Mechanistically, it causes cell cycle arrest from G1 to S phase by inhibiting the phosphorylation of the retinoblastoma protein and activating the E2F transcription factor. It is majorly involved in the treatment of

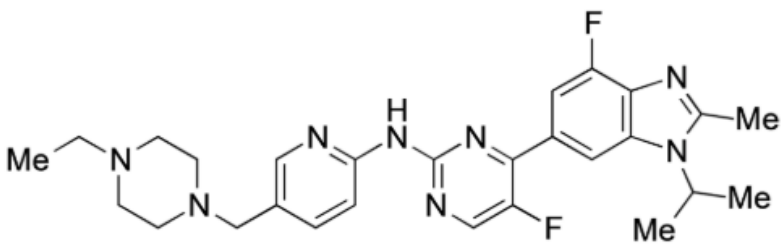

Figure 5.1: Chemical structure of Abemaciclib.

advanced or metastatic breast cancer in both combination therapy and monotherapy. But apart from breast cancer, currently being investigated for the treatment of other cancers [Martínez-Chávez et al., 2021].

In our previous research, we identified several FDA-approved compounds that competitively inhibited the activity of the *L. donovani* citrate synthase enzyme. Among these, Abemaciclib stood out as it effectively hindered the growth and proliferation of both promastigote and intra-macrophagic amastigote forms at micromolar concentrations while exhibiting minimal toxicity towards murine macrophages. However, the precise molecular mechanism driving the demise of the parasite remained unexplored. Therefore, the present study aims to delve into the molecular intricacies underlying parasitic death induced by Abemaciclib.

5.2 Materials & Methods

5.2.1 Materials

M199 Media, H2DCFDA, Propidium Iodide dye, and the Mitochondrial Membrane Potential Detection Kit were procured from Sigma-Aldrich (St. Louis, MO, USA). The FITC Annexin V/Dead Cell Apoptosis Kit, RPMI-1640 Media, and Giemsa were purchased from Invitrogen (Grand Island, NY, USA). Fetal Bovine Serum (FBS) was obtained from Hi-media. All compounds were purchased from med chem express. All the other chemicals used in the experiments were of the highest grade.

5.2.2 *L. donovani* and J774 A.1 cell culture maintenance

L. donovani cultures AG83 (MHOM/IN/1983/AG83) were maintained in M199 media (pH 7.4) supplemented with 10% heat-inactivated fetal bovine serum (FBS) and 1% penicillin-streptomycin antibiotic at 25°C. The parasites consistently passaged every 3-4 days. J774A.1 cell line (murine macrophage cells) was cultivated in RPMI-1640 media (pH 7.4) with 10% FBS, 1% penicillin-streptomycin, and gentamicin antibiotic at 37°C and 5% CO_2. The chemical stock was prepared in DMSO, followed by blank M199 media.

5.2.3 Morphological analysis of promastigote

L. donovani promastigote (2x 10^6 cells/ml) was incubated with IC_{50} and 2x IC_{50} of Abemaciclib for 48h. After incubation, cells were harvested and washed with 1x PBS (pH 7.4). The treated cells and control were fixed with Karnovasky fixative containing 2% paraformaldehyde and 2.5% glutaraldehyde at room temperature for 1 hour. Afterward, cells were washed with 1x PBS two times, and their moisture was removed by increasing the ethanol gradient. The dried sample was coated with a gold-palladium sputter coater and finally visualized in an LEO 435 electron microscope using an accelerating voltage of 15 kV [Ali et al., 2021]; [Islamuddin et al., 2022].

5.2.4 Analysis of mitochondrial integrity of promastigote

L. donovani promastigote (2x 10^6 cells/ml) was incubated with IC_{50} and 2x IC_{50} of Abemaciclib for 48 h at 25°C. After incubation, cells were harvested and washed with 1x PBS. The cells were resuspended in 100 nM MitoSoX red containing buffer and incubated for 30 min in the dark. After incubation, the cells were washed once with 1x PBS and resuspended in 1x PBS. The slides were observed under the Olympus fluorescence microscope to detect any abnormalities in the structure of the mitochondria [Antwi et al., 2019].

5.2.5 Analysis of ROS generation in promastigote

The IC_{50} and 2x IC_{50} doses of Abemaciclib treated and untreated promastigote were used in the reactive oxygen species (ROS) experiments [Saudagar and Dubey, 2014]. All cells were collected, rinsed twice with 1x PBS, and then incubated at room temperature for 30 minutes in the dark with 10 μM of cell-permeable 2,7-dichlorodihydrofluorescein diacetate acetyl ester (H2DCFDA) dye. All cells were then centrifuged at 3000 rpm for 10 min. The fluorescence intensity of each sample was recorded using a Backmann flow cytometer at 488 nm excitation and 522 nm emission wavelength, respectively, and analysis was done using Cyt expert

software. The histogram represented the two separate experiments and 100000 events acquired for each sample to ensure adequate data [Ali et al., 2021].

5.2.6 Analysis of mitochondrial membrane potential in promastigote

Parasites ($2*10^6$ cells/ml) were treated with IC_{50} and 2x IC_{50} doses of Abemaciclib and incubated for 48 hours at 25°C. After incubation, cells were collected and washed twice with 1x PBS. For positive control, untreated cells were incubated with 1 µl of 50 mM Carbonyl cyanide 3-chlorophenylhydrazone (CCCP) for 5 min., rinsed with 1x PBS once, and then samples were prepared as per manufacture instruction and examined under a BD FACSAria Flow cytometer using an excitation wavelength 488 nm and emission wavelength 505 to 550 nm (green) and 575 nm (red). The sample analysis was performed using BD FACSDiva software. The relative shift in the potential of the mitochondrial membrane was shown by the ratio of 590/530 (red/green) fluorescence. To guarantee adequate data, 10,000 events were collected for every sample. The dot plots represented the two separate studies [Ali et al., 2021],[Bortoleti et al., 2021].

5.2.7 Detection of chromatin condensation in promastigote

L. donovani promastigote ($2* 10^6$ cells/ml) was incubated with IC_{50} and 2x IC_{50} of Abemaciclib for 48 h at 25°C. After incubation, cells were harvested and washed once with 1x PBS. The cells were resuspended in Karnovasky fixative containing 2% paraformaldehyde and 2.5% glutaraldehyde for half an hour at 4°C. Afterward, cells were washed with 1x PBS two times. The cells were resuspended in 3µM DAPI containing buffer and incubated for 15 min in the dark. After incubation, the cells were washed once with 1x PBS and resuspended in 1x PBS. The slides were prepared and observed under the Olympus fluorescence microscope to detect any abnormalities in the structure of the mitochondria [Antwi et al., 2019].

5.2.8 DNA Laddering assay in promastigote

L. donovani promastigote (2 * 10^6/ml) was incubated with IC_{50} and 2X IC_{50} concentrations of abemaciclib for 48 hours to examine the DNA fragmentation. After incubation, cells were collected and placed in 0.5 ml of an extraction buffer containing RNAse, proteinase K, 0.5% SDS, 10 mM Tris-HCl, pH 8.0, and 100 mM EDTA. The mixture was vortexed and held at 50 °C for one hour to aid digestion. The lysates were extracted using phenol-chloroform-isoamyl alcohol (25:24:1 v/v) and centrifugation at 16000g for 10 minutes. The upper aqueous phase was collected and incubated with 3M sodium acetate and 100% ethanol overnight at -20°C. The following day, the supernatant was extracted after samples were centrifuged at 10,000 rpm for 10 minutes at 4°C. The pellets were washed with 70% ethanol using a centrifuge at 10,000 rpm for 10 minutes at 4°C. After discarding the supernatant, the DNA was disintegrated into nuclease-free water. DNA samples were placed into a 1.5% agarose gel, processed for 1.5 hours at 60 volts, and examined with a gel doc [Saudagar and Dubey, 2014].

5.2.9 Cell cycle analysis in promastigote

Parasites (2*10^6/ml) were incubated with IC_{50} and 2x IC_{50} doses of abemaciclib for 48 hours. After incubation, cells were collected, twice-washed in 1x PBS, fixed with 70% ethanol, and stored at 4 °C overnight. The fixed parasites were washed with 1x PBS, mixed with 100 µl of RNAse A (20 mg/ml), and incubated at 37 °C for 30 min. Furthermore, the samples were incubated with 50 µg/ml of propidium iodide (PI) at room temperature for 20 min in the dark before being rinsed once with 1x PBS. The proportion of cells in the G0, G1, S, and G2/M phases of the cell cycle was analyzed with the BD FACSAria flow cytometer using excitation and emission wavelengths of 488 nm and 636 nm, respectively, and their analysis was done using FCS Express software. To ensure data, a total of 10,000 events were collected for each sample. The histograms represented the three separate studies [Saudagar et al., 2013]; [Ali et al., 2021].

5.2.10 Determination of phosphatidylserine exposure and membrane integrity in promastigote

The parasites (2 *10^6/ml) were incubated with IC_{50} and 2x IC_{50} doses of abemaciclib for 48 hours. Afterward, cells were twice washed with 1x PBS and incubated with Annexin-V and PI dye according to the manufacturer's instructions. The labeled cells were analyzed using BD FACSAria flow cytometry using the FITC/PI channel, and analysis was done using BD FACSDiva software. For the acquisition of each sample, 10000 events were collected, and the proportion of live and dead cells was calculated. The dot plots represented the two separate experiments [Saudagar et al., 2013];[Islamuddin et al., 2022].

5.2.11 Statistical analysis

Each quantitative experiment was carried out in triplicate with three different experiments. The data were presented as the mean of the triplicate ± SEM. The statistical analysis was done using Origin Pro 2021 software, and groups were compared using one-way ANOVA, followed by Tukey's test. We considered p values > 0.05 to be statistically significant.

5.3 Results

5.3.1 Morphological analysis of Abemaciclib treated promastigote

Morphological changes are the key hallmarks of an early stage of apoptosis. In SEM analysis, we found that the 2x IC_{50} concentration of Abemaciclib-treated cells altered the size, shape, and length of the flagella, whereas untreated cells showed elongated bodies with long flagella at the anterior end, as shown in Figure 5.2.

5.3.2 Analysis of the effect of Abemacilcib on mitochondrial integrity of promastigote

We examined the impact of Abemaciclib at both IC_{50} and 2x IC_{50} concentrations on the mitochondrial structure by exposing promastigotes to the compound for 48 hours. Upon staining the parasites with MitoSox red, untreated parasites exhibited clearly defined

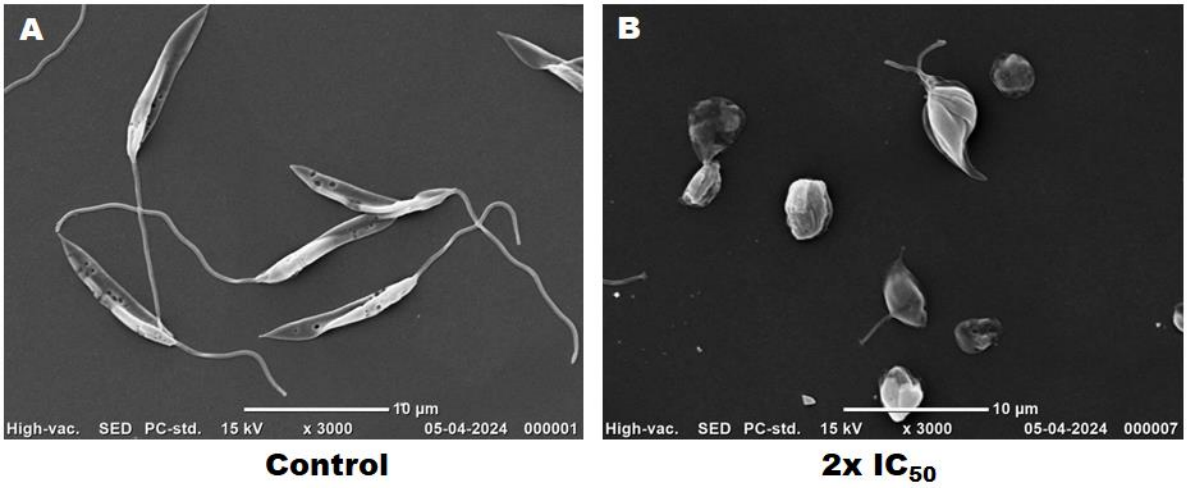

Figure 5.2: SEM micrograph of morphological changes induced by different concentrations of abemaciclib in *L. donovani*. (A) SEM micrograph of the untreated sample showing long flagella and elongated body. **(B)** SEM micrograph of 2x IC_{50} conc. of Abemacilcib-treated promastigote cells show short flagella and a round body.

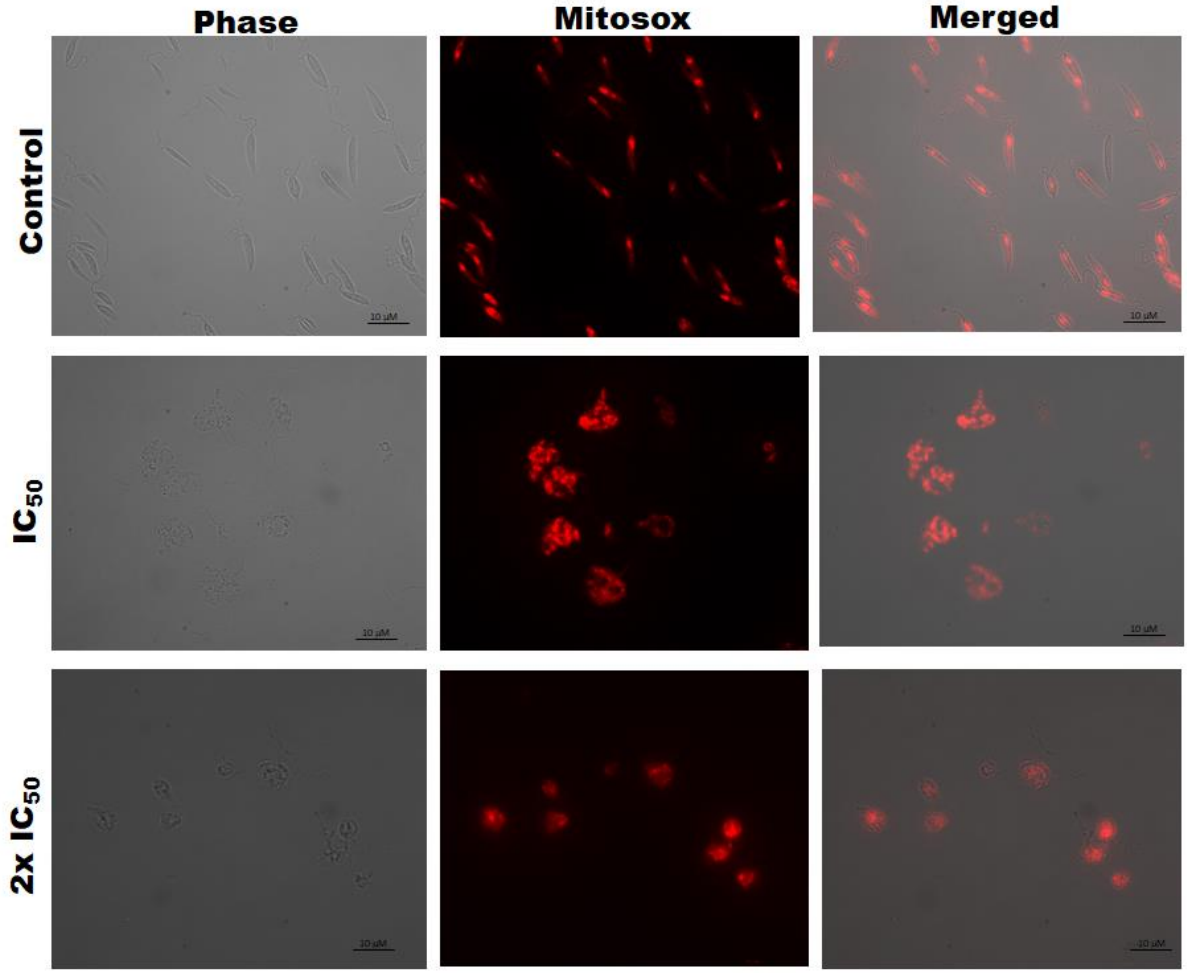

Figure 5.3: The phase contrast and fluorescence microscopy images of untreated and treated promastigote. The image of promastigote was taken after 48 h exposure of IC_{50} and 2x IC_{50} concentration of Abemaciclib and stained with MitoSox red.

mitochondria within the cell body. In contrast, parasites treated with varying concentrations of Abemaciclib displayed distorted mitochondria and accumulation of dye in the cytoplasm, forming bright red aggregations, as illustrated in Figure 5.3.

5.3.3 Abemaciclib induced ROS production in Promastigote

In various oxidative stress-related cellular processes, ROS induction plays a significant role. [Rani et al., 2022]. To evaluate the effect of abemaciclib on ROS generation in the parasite, H_2DCFDA staining was performed. In this study, a significant fluorescence shift was observed in the right direction at IC_{50} and 2x IC_{50} concentration, as shown in Figure 5.4 (I). At IC_{50} doses, there were 33% ROS positive cells, and at 2x IC_{50} doses, 48.72% ROS positive cells were found compared to the untreated control. In the case of positive control (50 µM H_2O_2), 61% ROS positive cell was found, as shown in Figure 5.4 (II). From this result, it can be concluded that this compound induced oxidative stress in mitochondria through ROS production.

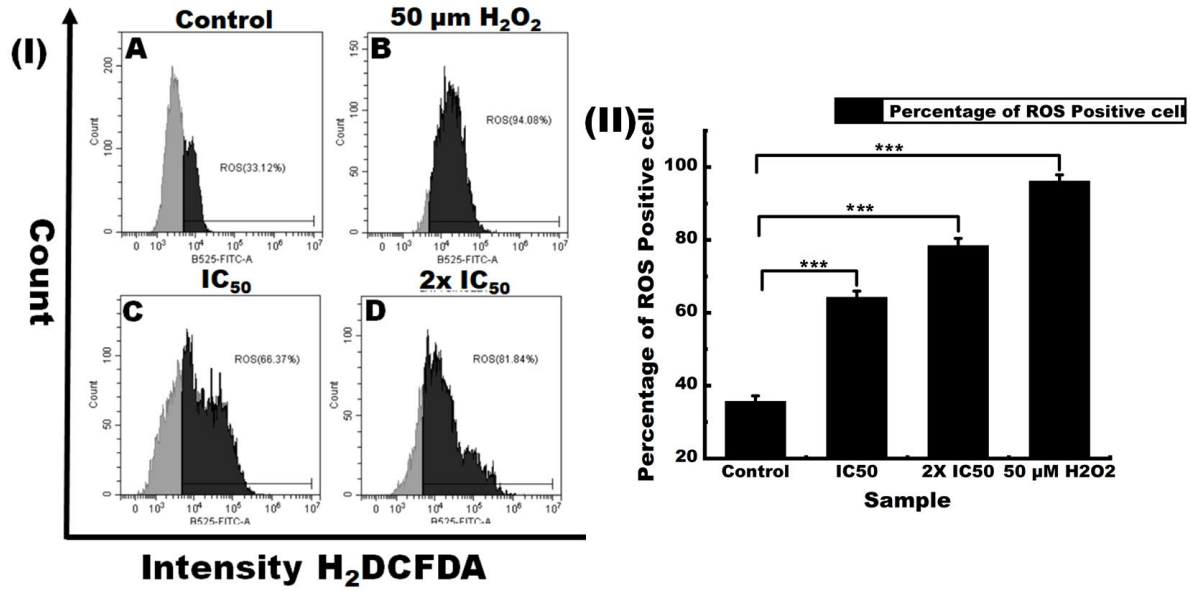

Figure 5.4: Abemaciclib induced ROS production in promastigote. (I)The dot plot shows ROS production in *L.donovani* promastigote after 48 hours of treatment, which was estimated by H_2DCFDA staining. A) untreated sample (-ve control) B), 50 µM H_2O_2 treated sample (+ve control), C) & D) IC_{50} and 2x IC_{50} dose of Abemaciclib treated sample. (II) Bar graph representing the percentage of ROS positive cells in an untreated sample, IC_{50}, 2x IC_{50}, and 50 µM H_2O_2. The graph represents the mean ± SEM of two different experiments in triplicate. Significant difference compared with the control * ($p < 0.01$), ** ($p < 0.001$), and *** ($p < 0.0001$).

5.3.4 Abemacilcib induced depolarization of mitochondrial membrane potential in promastigote

A hallmark of apoptosis is the lowering of the mitochondrial membrane potential [Saudagar et al., 2013]. To identify depolarization of the mitochondrial membrane potential, JC1 dye was added to the cells treated with IC_{50} and 2x IC_{50} of Abemaciclib. It is a cationic dye that is unique to mitochondria, which get aggregated in healthy mitochondria and produce red fluorescence but is unable to do so in unhealthy or depolarized mitochondria; thus, it gets accumulated in the cytosol in monomeric form, producing green fluorescence [Saudagar and Dubey, 2014]. At IC_{50} and 2x IC_{50} doses of abemaciclib, we found 46 and 32% of depolarized mitochondria compared to the untreated control in a flow cytometric study. In positive control (CCCP), 87% of the mitochondrial cells were depolarized, as shown in Figure 5.5 (I). Additionally, it was shown in Figure 5.5 (II) that the drug Abemacilcib caused a striking decline in the red-to-green

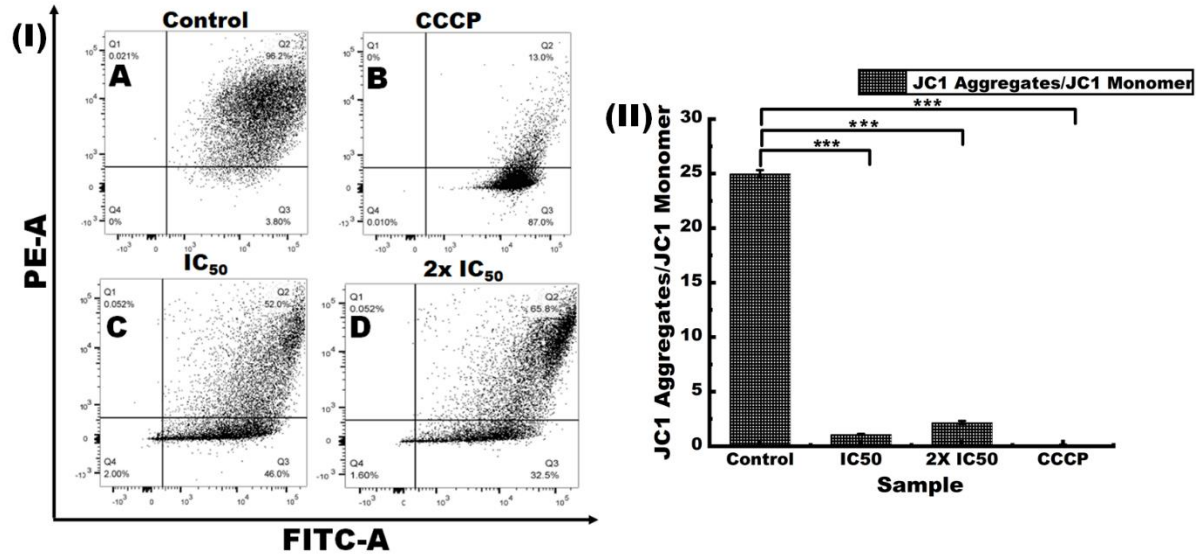

Figure 5.5: Abemaciclib induced depolarization of mitochondrial membrane potential in promastigote. (I) Dot plot showing shifting of fluorescence in the green channel (FITC-A), which was done in (A) Untreated sample (-ve control), (B) CCCP (+ve control), (C) & (D) IC_{50} and 2x IC_{50} doses of Abemaciclib treated sample after incubation with 48h and stained with JC-1 dye. Here, Normal mitochondrial membrane potential was shown by red fluorescence, and depolarized mitochondrial membrane potential was shown by green fluorescence. (II) The bar graph represents the JC1 aggregate and JC1 monomer ratio in the untreated sample (-ve control), CCCP (positive control), $IC_{50,}$ and 2x IC_{50} doses of Abemaciclib. The graph represents the mean ± STDEV of two different experiments in triplicate. Significant difference compared with the control * ($p < 0.01$), ** ($p < 0.001$), and *** ($p < 0.0001$).

fluorescence intensity ratio, which is a sign that the mitochondrial membrane had depolarized.

5.3.5 Analysis of the effect of Abemacilcib on the nuclear structure of promastigote

Leishmanial cells possess distinctive features, notably a large mitochondrion containing DNA composed of mini- and maxi-circles, which appears highly condensed and visible upon staining with DAPI [Basmaciyan et al., 2018]. Therefore, changes in the nuclear structure of parasites were examined following treatment with IC_{50} and 2x IC_{50} concentrations of Abemaciclib after 48 hours of incubation, followed by DAPI staining. In untreated parasites, the kinetoplast and nuclear DNA remained intact. However, parasites treated with the IC_{50} concentration of Abemaciclib exhibited aggregation of nuclear and kinetoplast DNA, while those treated with 2x IC_{50} concentration displayed enlargement of nuclear DNA and loss of kinetoplast DNA, as depicted in Figure 5.6.

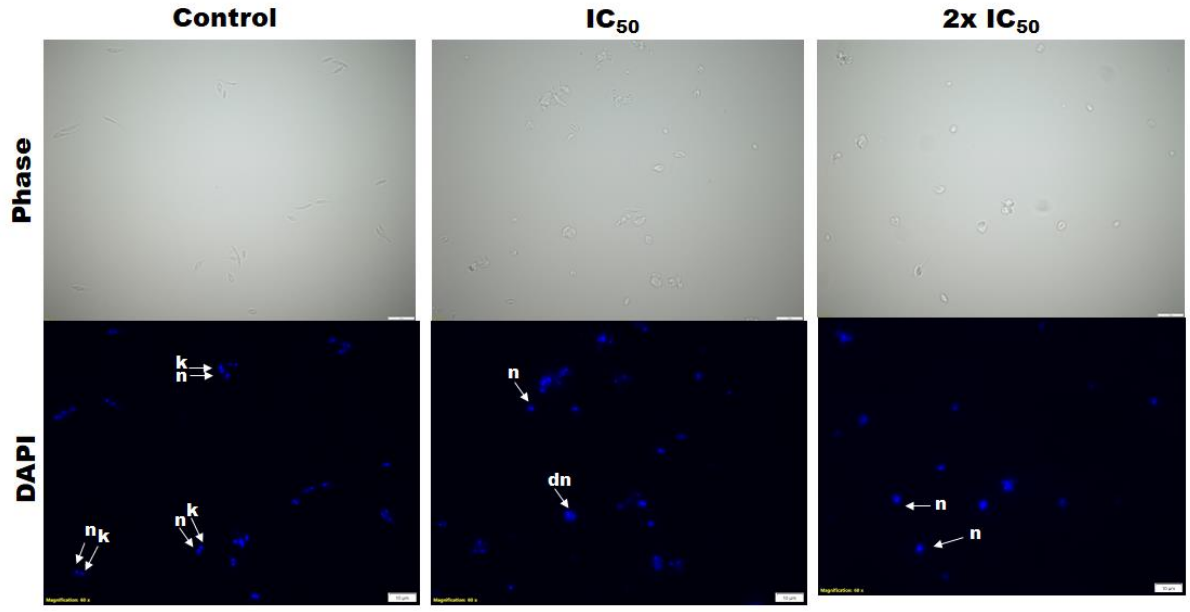

Figure 5.6: The images of promastigote after 48 h exposure of IC_{50} and 2x IC_{50} concentration of Abemaciclib and stained with DAPI, examined by Phase contrast and fluorescence microscopy at x60. **k= Kinetoplast; n= Nucleus**

5.3.6 Abemaciclib induced cell cycle changes in promastigote

To assess the effect of IC_{50} and 2x IC_{50} doses of Abemaciclib at various cell cycle phases, PI staining was done, and its analysis was performed by flow cytometry. In the analysis, it was found the population of G0-G1 and sub-G1 cells significantly decreased and increased concurrently in a dose-dependent fashion. The population of S phase and G2-M phase cells remained steady, as depicted in Figure 5.7 (I) [Keshav et al., 2023]. Compared to untreated control cells, the IC_{50} treated cells had 38%, and 2x IC_{50} treated cells had 44% sub G1 cell population, respectively, as depicted in Figure 5.7 (II).

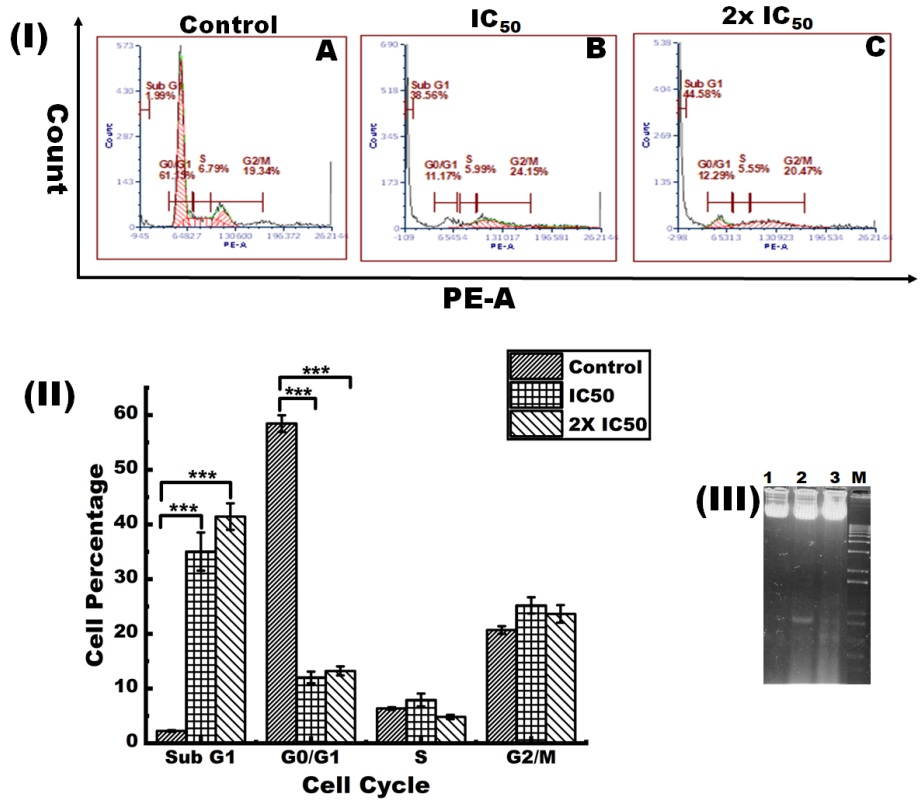

Figure 5.7: Cell cycle analysis and Genomic DNA fragmentation assay with Abemaciclib treated sample of promastigote.
(I)Dot plot showing the change in percentage of cells in different phases of the cell cycle, which was done in (A) Untreated sample (-ve control), (B) & (C) IC_{50} and 2x IC_{50} treated sample after 48 hours incubation and staining with propidium iodide dye. (II) The bar graph representing the quantification of cell cycle populations demonstrated that the proportion of cells increased in the sub-G1 phase of the Abemaciclib treated sample compared with the untreated sample. The graph represents the mean ± STDEV of two different experiments in triplicate. Significant difference compared with the control * ($p < 0.01$), ** ($p < 0.001$), and *** ($p < 0.0001$).
(III) Genomic DNA fragmentation in IC_{50} doses of Abemaciclib treated sample and compared with an untreated sample of promastigote, which had been done by agarose gel electrophoresis. Lane 1 represents the untreated sample, Lane 2 represents the IC_{50} dose of the Abemaciclib treated sample, Lane 3 represents the IC_{50} dose of the Miltefosine treated sample, and Lane M represents the DNA molecular mass marker ($1kb^{+}$ DNA ladder).

5.3.7 Abemaciclib induced Genomic DNA Fragmentation

Disintegration of genomic DNA is characterized as a hallmark of apoptosis. The genomic DNA fragmentation assay was performed on cells treated with IC50 doses of Abemaciclib, Miltefosine (a positive reference), and untreated cells using agarose gel electrophoresis. At IC_{50} dosages, Abemaciclib significantly fragmented the genomic DNA, as shown in Figure 5.7 (III), indicating that it occurs due to the activation of endonucleases [Ali et al., 2021].

5.3.8 Abemaciclib induced externalization of phosphatidylserine in the plasma membrane of promastigote

Externalization of phosphatidylserine (PS) is an established characteristic of apoptosis.

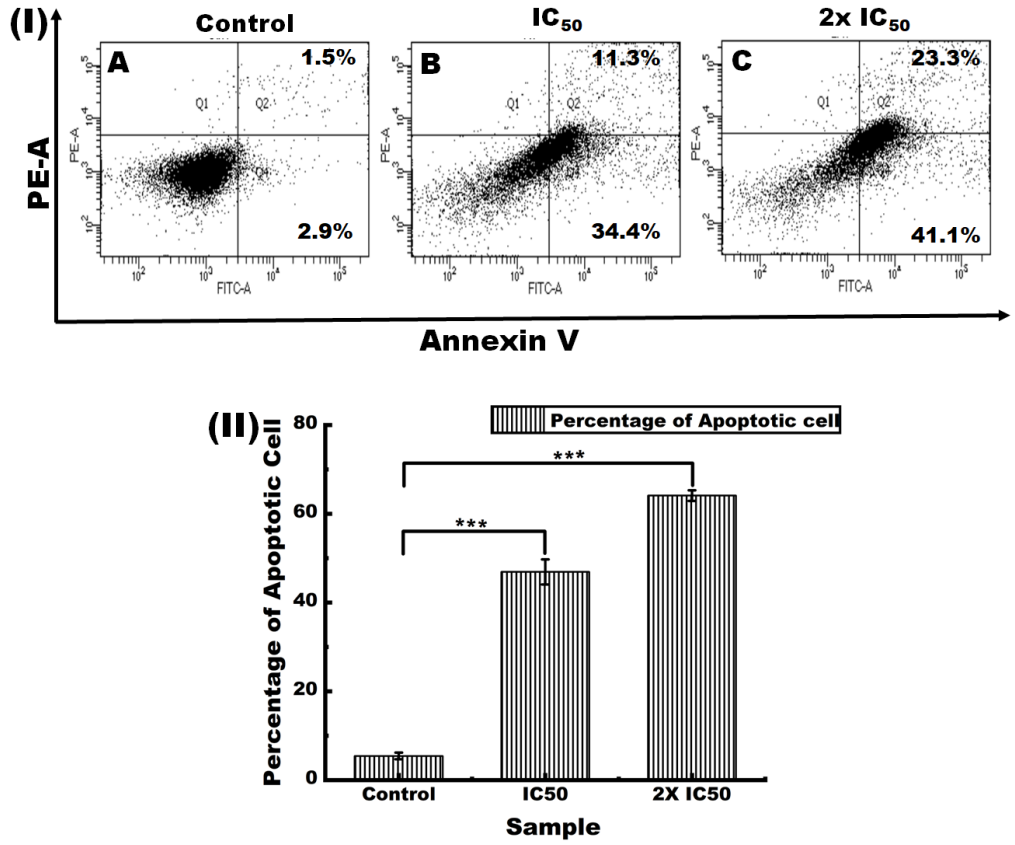

Figure 5.7: Abemaciclib induced apoptosis like cell death in promastigote. (I)Dot plot showing externalization of phosphatidylserine in (A) Untreated sample, (B) & (C) IC_{50} and 2x IC_{50} doses of Abemaciclib treated sample which have incubated for 48 hours and stained with annexin V and PI. (II) Bar graph representing the percentage of apoptotic cells in IC_{50} and 2x IC_{50} doses of Abemaciclib treated sample. The graph represents the mean ± STDEV of two different experiments in triplicate. Significant difference compared with the control * ($p < 0.01$), ** ($p < 0.001$), and *** ($p < 0.0001$).

It is detected by Annexin V dye since it has a strong affinity for phosphatidylserine. For screening of apoptotic and necrotic cells using flow cytometry, Abemaciclib IC_{50} and 2x IC_{50} treated cells were taken and double stained with Annexin V and Propidium Iodide (PI) dye. There were 34.4% of the parasites found in the early apoptosis and 11.3% in the late apoptosis at IC_{50} doses, whereas in 2x IC_{50} doses, there were 41.1% of the parasites in early apoptosis and 23.3% in late apoptosis. When increasing the dose from IC_{50} to 2x IC_{50}, parasites shifted from early to late apoptosis compared to untreated control, as shown in Figure 5.8 (I). Compared to untreated control, in IC_{50} doses of abemaciclib, there were 46% parasites, and in 2x IC_{50} doses, 64.4% parasites were found in the apoptotic state, as shown in Figure 5.8 (II). This work strongly suggested that Abemaciclib induces a cell death mechanism akin to apoptosis.

5.4 Discussion

In the contemporary landscape of medicine, drug repurposing has emerged as a commonly employed strategy for treating a multitude of diseases with efficacy. Notably, two key drugs utilized in the treatment of leishmaniasis, Miltefosine, and Amphotericin B, were initially formulated as anti-neoplastic and antifungal agents, respectively [da Silva Rodrigues et al., 2019]. Here, we have taken Abemaciclib, an anti-cancer drug, to repurpose against leishmaniasis. As data mentioned in the previous chapter, we observed the inhibitory effect of Abemacilcib at micromolar concentrations against both the promastigote and intra-macrophagic amastigote form of *L. donovani* without much toxicity as it has shown the excellent selectivity index against both forms of the parasite [Ranjan and Dubey, 2023b]. Its safety is further assured by the fact that it has long been used by general populations for the treatment of breast cancer. There are a few reports of antileishmanial activities of some compounds such as Miltefosine [Verma and Dey, 2004], Amphotericin B [Lee et al., 2002], Artemisinin [Dutta et al., 2007], Reacemoside [Sen et al., 2007] and Curcumin [Das et al.,

2008] was mediated through apoptosis. Apoptosis is a programmed cell death mode involving alteration in cellular morphogenesis and homeostasis. It is characterized by biochemical events such as membrane blebbing, chromatin condensation, cellular shrinkage, nuclear fragmentation, and mRNA decay [Islamuddin et al., 2022]. An earlier study on Abemacilcib proved that it exhibited significant cytotoxic and apoptotic effects against prostate cancer cells [Guney Eskiler et al., 2022]. In the present study, we attempted to illustrate the mechanism of antileishmanial activities of Abemacilcib against *L. donovani*. The Abemaciclib treated promastigotes showed a typical alteration in morphological patterns such as rounding, cytoplasmic shrinkage, loss of flagella, and membrane blebbing observed under scanning electron microscopy, showing earlier evidence of apoptosis. Further, we focused on mitochondria, a key cellular organelle that is crucial for both cell survival and energy metabolism. Citrate synthase, which is the main focus of this research, is also present in the mitochondrial matrix. Therefore, it's possible that a citrate synthase inhibitor will have an impact on the mitochondria. The structure of mitochondria in the treated sample was analyzed by MitoSoX red, which showed the distortion of well-defined mitochondrion and accumulation of dye in the cytoplasm with bright red aggregation. We examined the ROS production in leishmania promastigote treated with IC_{50} and 2x IC_{50} dosages of Abemaciclib. A dose-dependent pattern of 33% to 50% ROS positive cells were observed. High levels of ROS production can result in mitochondrial malfunction, as evidenced by the striking drop in JC-1 dye's red/green fluorescence intensity. Apoptotic eliciting signals are released by the damaged mitochondrial membrane, which activates the chain of caspase-like proteases and causes genomic DNA fragmentation and apoptosis [Saudagar and Dubey, 2014]. In leishmania promastigotes, Abemaciclib-induced genomic DNA fragmentation was seen. When compared to untreated samples (1.99%), IC_{50} and 2x IC_{50} dosages of Abemaciclib-treated samples revealed a sub-G1 cell population of 38.56% to 44.58%, further indicating the promastigote's

apoptotic mode of death mechanism [Murad et al., 2016]. For further confirmation of apoptotic like cell death mechanism, the treated leishmania promastigotes were doubled stained with Annexin V-FITC and PI. AnnexinV has affinity for phosphatidylserine which basically occur in apoptotic cells whereas PI has for necrotic cells. Normal cells do not have an affinity for both dyes. Based on this, in IC50 and 2x IC50 doses, 46% and 64% of parasites were found in the apoptotic state [Saudagar and Dubey, 2014]. In apoptosis like death mechanism, generally we observed cell shrinkages, cell membrane blebbing, depolarization of mitochondrial membrane potential, genomic DNA fragmentation, cell cycle arrest and PS externalization [Ali et al., 2021]. We had also observed all those phenomena in our Abemaciclib treated leishmania promastigote sample. Based on above result, it is strongly envisaged that our repurposed compound Abemaciclib will be a promising antileishmanial medication.

5.5 Conclusion

The current study highlights the potential repurposing of the anticancer drug Abemaciclib for leishmaniasis treatment. Recognizing the intricate interplay and complexity of cell death mechanisms in trypanosomatids, we sought to elucidate the mode of action of Abemaciclib. Our findings reveal that Abemaciclib targets the promastigote form of Leishmania by inducing ROS generation, mitochondrial membrane potential loss, nuclear condensation, DNA fragmentation, cell cycle arrest, and phosphatidylserine externalization, collectively indicative of an apoptosis-like cell death mechanism. Pending further testing and validation, these compounds hold promise as effective antileishmanial agents against this debilitating disease.